Journal of Physics D: Applied Physics

PAPER

Toroidal dipole response in the individual silicon hollow cylinder under radially polarized beam excitation

To cite this article: Jiawei Xu *et al* 2021 *J. Phys. D: Appl. Phys.* **54** 215102

IOP Publishing Journal of Physics D: Applied Physics
J. Phys. D: Appl. Phys. **54** (2021) 215102 (6pp) https://doi.org/10.1088/1361-6463/abe66c

Toroidal dipole response in the individual silicon hollow cylinder under radially polarized beam excitation

Jiawei Xu, Haihua Fan, Qiaofeng Dai, Haiying Liu and Sheng Lan

Guangdong Provincial Key Laboratory of Nanophotonic Functional Materials and Devices, School of Information and Optoelectronic Science and Engineering, Guangzhou 510006, People's Republic of China

E-mail: hyliu@scnu.edu.cn

Received 4 December 2020, revised 3 February 2021
Accepted for publication 15 February 2021
Published 3 March 2021

Abstract

The toroidal dipole (TD) has attracted growing attention due to its unique properties. Here, we propose and demonstrate almost pure TD resonance in the visible region in a silicon hollow cylinder. The enhanced optical coupling to TD resonance is implemented using a focused radially polarized beam illumination matching, well-designed individual silicon nanostructure resonator. The polarization of the longitudinal electric field in the silicon hollow cylinder that breaks space-inversion symmetry is critical to the formation of enhanced TD resonance. Additionally, the pure TD resonance can be achieved in a wide spectral range by tuning the geometrical parameters of the structure. The proposed pure TD resonator may provide potential applications in the local enhancement of electromagnetic fields and the design of all-dielectric nanoantennas.

Keywords: toroidal dipole resonance, radially polarized beam, all-dielectric resonator

(Some figures may appear in colour only in the online journal)

1. Introduction

The toroidal dipole (TD), as the simplest member of the toroidal multipole family, characterized by a vortex distribution of magnetic dipoles, was first proposed by Zel'dovich in 1957 to interpret the parity violation in weak interactions [1, 2]. A magnetic (polar) TD corresponds to a current circulating on a surface of a toroid along its meridians [3]. So far, various promising functions have been demonstrated in the presence of TD modes, such as directional scattering of light [4, 5], enhanced optical nonlinearity [6], metasurfaces [7–11], etc. For a long time, the TD has been unfortunately neglected by researchers because of their weak coupling to incident light, the same far-field radiation as the electric dipole (ED) and because the Taylor expansion of the displacement current under the large-wavelength approximation involves complex tensor derivations [12, 13]. Since the TD resonance was experimentally observed on microwave metal metamaterials for the first time in 2010 [3], however, people have carefully designed specific metamaterials to enhance the TD resonance [14–17]. But these various metal resonators capable of supporting a TD response usually have a very complex shape, so they are difficult to manufacture on the nanometer scale. Another severe problem is the non-negligible ohmic losses of metal metamaterials at optical frequencies. High refractive index dielectric metamaterials with low loss characteristics can also support TD mode by forming an out-of-phase displacement current.

Some studies focused on the realization of the dominant TD resonance in all-dielectric nanostructures. For example, strong TD resonance was achieved by introducing the trap mode in asymmetric dielectric quadrumer clusters [18, 19]. Besides that, it is demonstrated that a permittivity-asymmetric dielectric metasurface based on a quadrumer structure, which allows for the excitation of strong TD responses at the near-infrared spectral ranges [20]. They can be summarized as using the asymmetry of the clusters structure (or refractive index) to enhance TD resonance. The enhancement of TD resonance in a single symmetrical nanostructure is still challenging. In

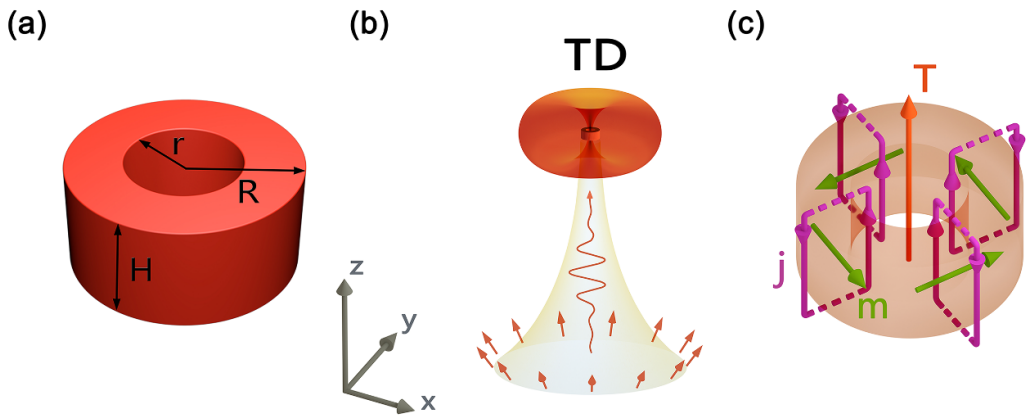

Figure 1. Schematic diagram of (a) the Si hollow cylinder and (b) TD resonance excited by a focused radially polarized beam. (c) The near-field current configuration of the hollow cylinder at resonances. Purple arrows show displacement currents excited by the incident light, green arrows show magnetic dipole moments m, and the red arrow represents the toroidal dipole moment T.

addition, as a high-order resonance, TD resonance is not only very weak, but also will overlap with other multipole resonance [21]. In the above studies, linearly polarized light is used as the excitation light source, which will inevitably introduce magnetic resonance. It is well known that the TD with a unique ring magnetic field is very necessary to control the local electromagnetic field. The enhancement of local electromagnetic field depends on the different topology of charge-current excitations. Pure TD can avoid the influence of the charge-current distribution of other multipoles. Therefore, the research on the enhanced pure TD resonance has become a popular topic.

In this paper, we propose an all-dielectric Si hollow cylinder (HC) that can achieve enhanced pure TD resonance. A focused radially polarized beam (RPB) is utilized as the incident light source. At each point, the electric field of the RPB is linearly polarized but its vector is oriented parallelly to the radius vector from the beam axis. The RPB has the capability to effectively excite TD resonance and suppress magnetic resonance in a symmetrical nanostructure. In this way, the TD resonance of the Si HC can be excited effectively, resulting in the generation of the enhanced pure TD resonance. We have demonstrated that an enhanced pure TD resonance can be achieved in a Si HC excited by an RPB. It is shown that the enhanced pure TD resonance originates from the polarization of the longitudinal electric field of the RPB. The wavelength as well as intensity of the TD resonance can be adjusted effectively in a wide spectral range by tuning the geometrical parameters of the HC. In addition, the electric hot spot can be observed at TD resonance wavelength, and electric field is localized in the hollow part of the cylinder, which can be accessed by external probes. The enhanced pure TD may provide new ideas for facilitating the light–matter interaction and designing all-dielectric nanoantennas.

2. Design and results

In figure 1(a), the height of the HC is $H = 150$ nm and the inner and outer radius are $r = 80$ nm and $R = 160$ nm, respectively. Figure 1(b) graphically shows the TD resonance of the Si HC excited by a focused RPB. In figure 1(c), the near-field current configuration of the HC at TD resonance is visually displayed. Purple arrows show displacement currents excited by the incident light, green arrows show magnetic dipole (MD) moments m and the red arrow represents the TD moment T. In order to obtain the contribution of the TD resonance to the total scattering power spectrum, we adopted a Cartesian multipole decomposition method for scattered light from arbitrary shape scatterers [22]. The multipole moment originates from the polarization $P(r) = \varepsilon_0(\varepsilon_p - \varepsilon_d)E(r)$ induced by the incident light, where $E(r)$ is the total electric field inside the scatterer. ε_0, ε_p and ε_d are the free-space dielectric constant, relative permittivity of the nanoparticle and relative permittivity of the surrounding medium, respectively. The multipoles locate at the origin of the Cartesian coordinate system according to the scatterer's center of mass. At this time, the ED moment can be expressed as:

$$p = \int_V P(r')\mathrm{d}r' \tag{1}$$

where V is the volume of the scatterer and r' is the radius vector of the volume element inside the scatterer. The TD moment is written as:

$$T = \frac{i\omega}{10}\int_V \left\{2r'^2 P(r') - [r'\cdot P(r')]\,r'\right\}\mathrm{d}r'. \tag{2}$$

The MD moment of the scatterer is described as:

$$m = -\frac{i\omega}{2}\int_V [r'\times P(r')\,\mathrm{d}r']\,. \tag{3}$$

The irreducible electric quadrupole (EQ) and magnetic quadrupole (MQ) tensors are written as ($\hat{U}$ is the 3×3 unit-tensors):

$$\hat{Q} = 3\left[\int_V r'\,P(r') + P(r')\,r' - \frac{2}{3}(r'\cdot \mathrm{P}(r'))\,\hat{U}\right]\mathrm{d}r' \tag{4}$$

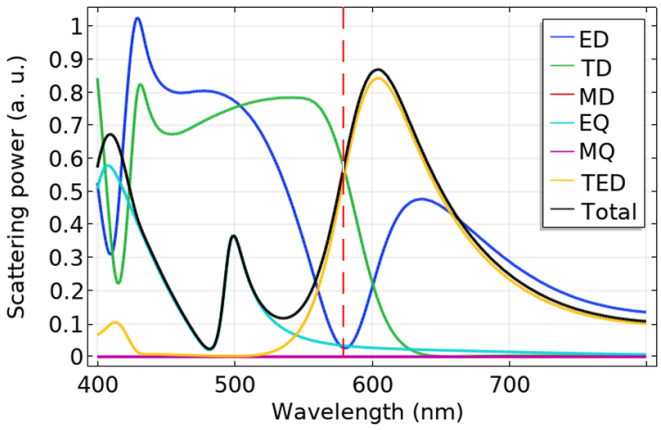

Figure 2. Multipole decomposition of the far-field scattering power spectrum of the Si hollow cylinder. Various electric and magnetic modes (up to the quadrupole) are obtained. The total scattering power (total) includes the contributions of TED, MD, EQ and MQ.

$$\hat{M} = -\frac{i\omega}{3}\int_V \{[r' \times P(r')]\, r' + r'\,[r' \times P(r')\,\mathrm{d}r']\}. \tag{5}$$

The total electric dipole (TED) moment is given by:

$$D = p + \frac{ik_0}{c}\varepsilon_d \mathrm{T} = p + \frac{ik_0}{c}T. \tag{6}$$

Finally, considering all the above mentioned multipole moments, the total far-field scattering power P_{sca} is written as:

$$P_{\mathrm{sca}} \cong \frac{k_0^4}{12\pi\varepsilon_0^2\nu_d\mu_0}\left|p + \frac{ik_d}{\nu_d}T\right|^2 + \frac{k_0^4\varepsilon_d}{12\pi\varepsilon_0\nu_d}|m|^2 + \frac{k_0^6\varepsilon_d}{1440\pi\varepsilon_0^2\nu_d\mu_0}\sum_{\alpha\beta}|Q_{\alpha\beta}|^2 + \frac{k_0^6\varepsilon_d^2}{160\pi\varepsilon_0\varepsilon_0\nu_d}\sum_{\alpha\beta}|M_{\alpha\beta}|^2 \tag{7}$$

where, $\alpha = x, y, z$, $\beta = x, y, z$, μ_0 is the vacuum permeability and ν_d is the light velocity in the surrounding medium; k_0 and k_d are the wave numbers in the vacuum and same surrounding media, respectively. In our simulation, the cylindrical vector light propagates along the z-axis direction and is focused at the center of the HC. The focal field of the cylindrical vector beam as a excitation source is calculated using COMSOL Multiphysics in the frequency domain. The setting of the light source is referred to [23]. The numerical aperture NA of the objective lens used for focusing is 1.32, and the refractive index between the lens and the sample is 1.518, which corresponds to a focusing angle of $\pm 60°$. The HC is placed in a homogeneous air medium with $\varepsilon_d = 1$, while the relative dielectric constant of Si comes from Aspnes [24]. In fact, the substrate has to be introduced into the structure for fabricating the sample experimentally. Taking silica as the substrate, the spectral features of the given nanostructure remain unchanged, while all resonances acquire some red shift along the wavelength scale. Similar results have been shown in other studies [18, 20].

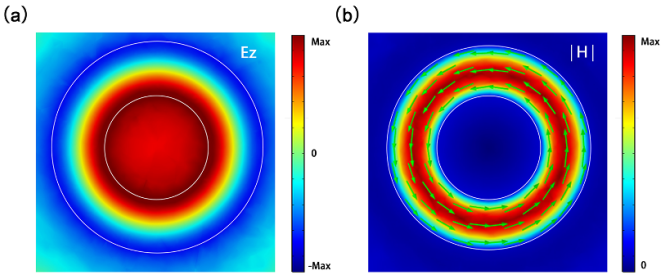

Figure 3. Distribution of the electromagnetic field in the xy plane of a hollow cylinder excited by a radially polarized beam at the TD resonance (580 nm) (a) electric field z component E_z, (b) magnetic field intensity $|H|$. Green arrows represent directions of the magnetic field.

From the multipole decomposition of the scattering power spectrum of the Si HC shown in figure 2 under the RPB illumination, we can find that the electric mode is selectively excited and all magnetic modes are suppressed. The MD and quadrupole moment is almost zero. This phenomenon can be explained by the multipole theory for tightly focused RPB reported in previous work [25]. A focused RPB is able to obtain a longitudinal electric field component along the propagation axis in the focus plane and its transverse electric field component is symmetrical. The polarizations excited by this symmetrical field distribution will cancel each other out in the symmetrical structure, so only the polarization caused by the longitudinal electric field is left. The focused RPB selectively coupling electric multipole resonances provides a tool for us to tailor TD mode. The results show that at a wavelength of about 580 nm (marked by a dashed line in figure 2), a dominant TD resonance is confirmed, which is usually weak in a single symmetrical structure. At the TD resonance wavelength, the weak contribution of ED can be understood as the result of mode competition. This is because both ED and TD are produced by the longitudinal electric field polarization of the RPB, and who gets the advantage depends on the wavelength relative to the radius of the resonator. In addition, an almost perfect EQ and TED were obtained at 499 nm and 605 nm, respectively. They originate from destructive and constructive interference of ED and TD, respectively.

We have plotted the near-field distribution of the electromagnetic field excited at the TD resonance, as shown in figures 3(a) and (b). Figures 3(a) and (b) correspond to the excited electric field E_z and magnetic field intensity $|H|$, respectively. The field distribution in figure 3(a) shows that the electric field E_z confined to the inner sidewall of the HC is along the positive z-axis direction, while the electric field E_z outside is along the negative z-axis direction. The parallel electric field E_z in different directions is caused by the parallel displacement current j flowing in the opposite direction. The formation of the antiparallel displacement current marked in figure 1(c) means that the symmetry of space-inversion is broken.

It is well known that TD break time-reversal and space-inversion symmetries simultaneously [13], so the formation of antiparallel displacement current is very important for the

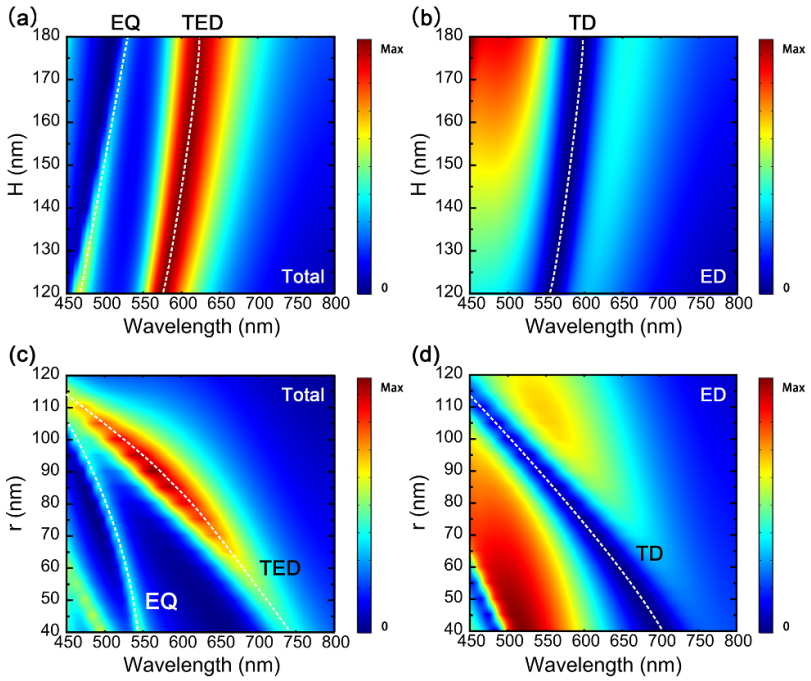

Figure 4. A hollow cylinder with an outer radius of $R = 160$ nm and an inner radius of $r = 80$ nm under the excitation of a radially polarized beam. A contour plot of (a) the total scattering power (b) the ED contribution as a function of wavelength and height H. A hollow cylinder with $R = 160$ nm and $H = 150$ nm under the irradiation of a radially polarized beam. A contour plot of (c) the total scattering power (d) the ED contribution as a function of wavelength and inner radius r.

excitation of TD resonance. This distribution of displacement current can generate a closed magnetic field vortex localized inside the HC, as shown in figure 3(b). The unique distribution of the above excitation fields confirms the TD mode. Interestingly, a strong electric field is localized in the center of the HC, which is confined to a small area by the magnetic field vortex. This local field, accessible by the near-field probes, facilitates its use in combination with a gain medium. Meanwhile, the Si HC can be regarded as a magnetic ring unit at the TD resonance wavelength. Such a magnetic vortex structure applies to many domains of science dealing with the enhancement of local electromagnetic fields.

In order to obtain pure TD resonances in a wider wavelength range, we discuss the modulation of the geometric parameter on the resonance. We first consider the total scattering power and the contribution of ED as a function of the wavelength at various heights under the irradiation of RPB, as shown in figures 4(a) and (b), respectively. TED is indicated by a dashed line in figure 4(a), and under the condition of ED ≈ 0, a dominant TD can be obtained. In figure 4(b), ED ≈ 0 is marked with a dashed line, and an almost pure TD can be obtained at this time. We found that with the increase of H, the TD resonance peak redshifted slightly, while the resonance intensity hardly changed, because H is not the main factor affecting the formation of the antiphase displacement currents. Figures 4(c) and (d) show the modulation of TD by r in the range of 40–120 nm. It should be noted that when $r > 85$ nm, the EQ peak will gradually couple with the TED peak, which is not conducive to obtaining pure TD. When $r < 60$ nm, too narrow hollow cylindrical wall will greatly reduce the antiphase oscillations of displacement currents, and the TD resonance intensity will be affected accordingly. If we adjust r in the range of 60–80 nm, we will get a dominant TD with a resonance peak in 580–680 nm.

It is known that the RPB excitation is highly dependent on the alignment of the structure center and the focal field. The parameter Δ is introduced to specify the lateral distance between the focus of the RPB and the center of the nanostructure. Figure 5(a) shows the scattering power spectrum when the offset distance $\Delta = 40$ nm. As can be seen from figure 5(a), MD and MQ resonances appear. This is because once the focus of the RPB shift away from the center of the structure, the polarization caused by the lateral excitation electric field of the RPB cannot cancel each other out. However, the influence of magnetic mode on the purity of TD can be controlled within a certain range. We further calculated the percentage of TD resonance to the total scattering power at the wavelength of ED resonance valley for different offset distance Δ, as shown in figure 5(b). We can obtain a TD resonance that accounts for more than 90% of the total scattering power as long as the offset distance Δ is within 40 nm.

Next, we kept the geometric parameters of the nanostructures unchanged and tried to replace the original focused RPB with the focused azimuthally polarized beam (APB). Interestingly, an almost pure MD resonance was obtained in a certain wavelength range. Under the illumination of the APB, MD (solid red line), MQ (solid purple line) and total scattering power (solid black line) are shown in figure 6(a), while TED and EQ scattering power are almost zero, which can safely be ignored. Although there is a weak MQ resonance

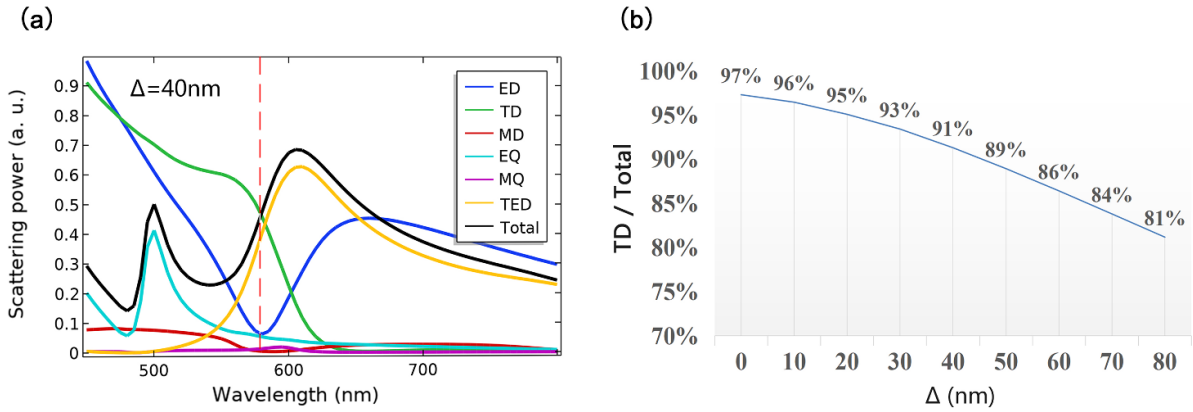

Figure 5. (a) Multipole decomposition of the far-field scattering power spectrum of the Si hollow cylinder when the offset distance $\Delta = 40$ nm (b) the percentage of TD resonance to the total scattering power for different offset distance Δ.

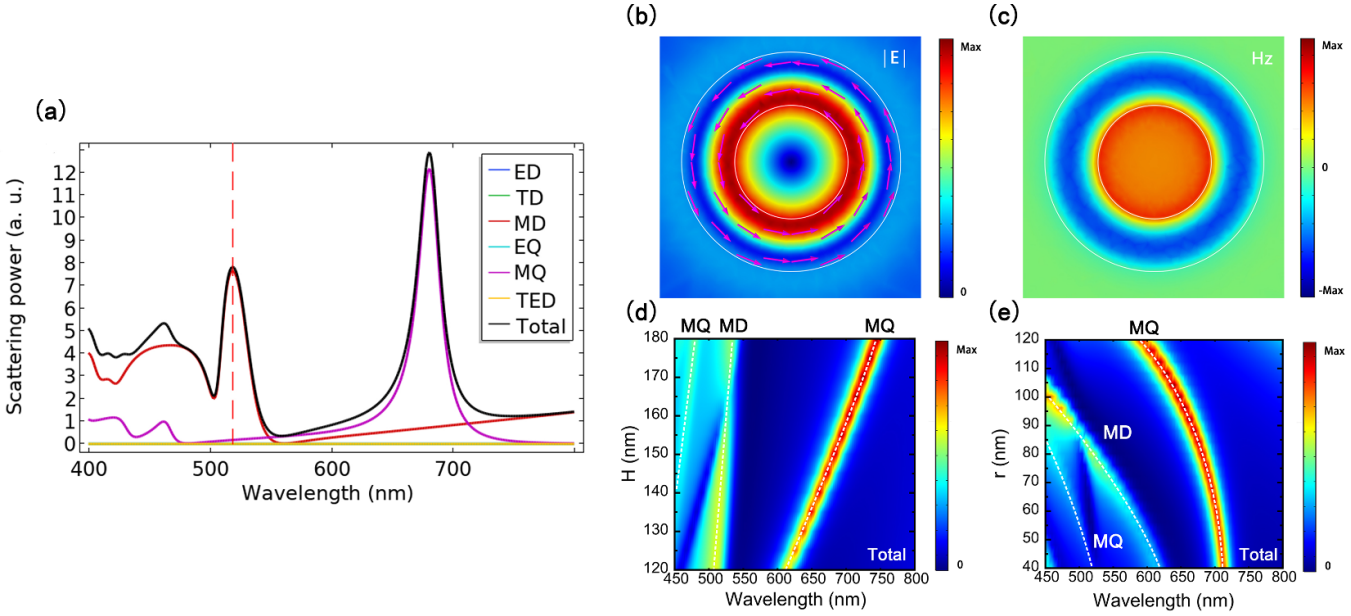

Figure 6. (a) Multipole decomposition of the scattering power spectrum using focused azimuthally polarized beam source. Electromagnetic field distribution diagram of *xy* plane of hollow cylinder at MD resonance (519 nm) (b) electric field intensity $|E|$, purple arrows represent directions of the electric field (c) *z* component of magnetic field. Under the illumination of an azimuthally polarized beam, a contour plot of the total scattering power (d) varying hollow cylinder heights H while keeping $R = 160$ nm and $r = 80$ nm, and (e) different inner radius while keeping $R = 160$ nm and $H = 150$ nm.

at the characteristic wavelength of 519 nm (marked by the red dashed line in figure 6(a)), the MD mode plays a major role in the total scattering power. In figures 6(b) and (c), the ring-shaped electric field distribution of the MD resonance and the magnetic hot spot in the hollow part of the cylinder are clearly observed. Similarly, the modulation of the MD resonance by H and r under the excitation of AP light is shown in figures 6(d) and (e), respectively. It can be seen from figure 6(d) that with the increase of H, the MQ at the shorter wavelength will be strengthened to couple with the MD to form a broadband resonance. As H decreases, the bandwidth of the MD increases. So, in order to maintain the purity of MD and high Q factor, $H = 150$ nm is a suitable parameter. Figure 6(e) shows that the inner diameter r has a wider modulation for the MD resonance wavelength. By maintaining $H = 150$ nm and adjusting the size of r to 60–80 nm, we can achieve a pure and high Q-factor MD resonance in the range of 520–580 nm. Similar results have been shown in other systems such as core–shell nanosphere and metal–dielectric–metal hybridized nanodisks [26, 27]. Pure MD excitation is of great significance for the unambiguous study of magnetic light-matter interactions.

3. Conclusions

In summary, we used the RPB to excite the Si HC, and obtained enhanced pure TD resonance, while other multipoles were suppressed. We find that the enhanced pure TD resonance is related to the formation of the out-of-phase displacement current excited by the longitudinal electric field of the focused

RPB. At the same time, at the TD resonance wavelength, there is an accessible electric hot spot in the hollow part of the cylinder. The localized electric field has a longitudinal component along the z-axis. Besides, the geometric parameters of Si HC have been explored for the modulation of TD resonance. Selecting the appropriate geometric parameter can achieve the dominant TD resonance in the range of 580–680 nm. The alignment error in the experiment is also considered, we can obtain a TD resonance that accounts for more than 90% of the total scattering power as long as the offset distance Δ is within 40 nm. In addition, we have made an extension to switch the light source to realize the pure MD mode. Our results may provide a useful platform for realizing efficient light–matter interaction for energy harvesting, nonlinear response, and data storage.

Acknowledgments

This work was supported by the Science and Technology Program of Guangzhou (Grant No. 2019050001); the Natural Science Foundation of Guangdong Province, China (Grant Nos. 2016A030308010, 2018A030313854 and 2019A1515011578); the National Nature and Science Foundation of China (Grant Nos. 11674110 and 11874020).

ORCID iD

Haiying Liu https://orcid.org/0000-0002-5280-1892

References

[1] Papasimakis N, Fedotov V, Savinov V, Raybould T and Zheludev N 2016 *Nat. Mater.* **15** 263
[2] Zel'Dovich I B 1957 *J. Exp. Theor. Phys.* **33** 1531
[3] Kaelberer T, Fedotov V, Papasimakis N, Tsai D and Zheludev N 2010 *Science* **330** 1510
[4] Terekhov P, Baryshnikova K, Shalin A, Karabchevsky A and Evlyukhin A 2017 *2017 Progress in Electromagnetics Research Symp.—Spring (PIERS)* vol 42, p 2325
[5] Deng F, Liu H-F, Panmai M-C and Lan S 2018 *Opt. Express* **26** 20051
[6] Ahmadivand A, Semmlinger M, Dong L, Gerislioglu B, Nordlander P and Halas N J 2018 *Nano Lett.* **19** 605
[7] Algorri J F, Zografopoulos D C, Ferraro A, García-Cámara B, Vergaz R, Beccherelli R and Sánchez-Pena J M 2019 *Nanomaterials* **9** 30
[8] Basharin A A, Kafesaki M, Economou E N, Soukoulis C M, Fedotov V A, Savinov V and Zheludev N I 2015 *Phys. Rev.* X **5** 011036
[9] He Y, Guo G, Feng T, Xu Y and Miroshnichenko A E 2018 *Phys. Rev.* B **98** 161112
[10] Sayanskiy A, Danaeifar M, Kapitanova P and Miroshnichenko A E 2018 *Adv. Opt. Mater.* **6** 1800302
[11] Xu S, Sayanskiy A, Kupriianov A S, Tuz V R, Kapitanova P, Sun H B, Han W and Kivshar Y S 2019 *Adv. Opt. Mater.* **7** 1801166
[12] Savinov V, Fedotov V and Zheludev N I 2014 *Phys. Rev.* B **89** 205112
[13] Gurvitz E A, Ladutenko K S, Dergachev P A, Evlyukhin A B, Miroshnichenko A E and Shalin A S 2019 *Laser Photon. Rev.* **13** 1800266
[14] Huang Y-W, Chen W T, Wu P C, Fedotov V, Savinov V, Ho Y Z, Chau Y-F, Zheludev N I and Tsai D P 2012 *Opt. Express* **20** 1760
[15] Bao Y, Zhu X and Fang Z 2015 *Sci. Rep.* **5** 11793
[16] Liu L, Ge L, Hu P, Xiang H, Yang W, Liu Q and Han D 2018 *J. Phys. D: Appl. Phys.* **51** 035106
[17] Hu P, Liang L, Ge L, Xiang H and Han D 2019 *J. Opt.* **21** 055001
[18] Tuz V R, Khardikov V V and Kivshar Y S 2018 *ACS Photonics* **5** 1871
[19] Zhang Z, Yang Q, Gong M and Long Z 2019 *J. Phys. D: Appl. Phys.* **53** 075106
[20] Liu X, Li J, Zhang Q and Wang Y 2020 *Opt. Lett.* **45** 2826
[21] Liu W, Zhang J, Lei B, Hu H and Miroshnichenko A E 2015 *Opt. Lett.* **40** 2293
[22] Evlyukhin A B, Fischer T, Reinhardt C and Chichkov B N 2016 *Phys. Rev.* B **94** 205434
[23] Youngworth K S and Brown T G 2000 *Opt. Express* **7** 77
[24] Aspnes D E and Studna A 1983 *Phys. Rev.* B **27** 985
[25] Hoang T X, Chen X and Sheppard C J 2012 *J. Opt. Soc. Am.* A **29** 32
[26] Feng T, Xu Y, Zhang W and Miroshnichenko A E 2017 *Phys. Rev. Lett.* **118** 173901
[27] Zhang Y, Yue P, Liu J-Y, Geng W, Bai Y-T and Liu S-D 2019 *Opt. Express* **27** 16143